PERGAMON

International Journal of Solids and Structures 40 (2003) 3157–3175

INTERNATIONAL JOURNAL OF SOLIDS and STRUCTURES

www.elsevier.com/locate/ijsolstr

Twin-characteristic-parameter solution of axisymmetric dynamic plastic buckling for cylindrical shells under axial compression waves

Anwen Wang *, Wenying Tian

Teaching and Research Section of Material Mechanics, The Naval Academy of Engineering, P.O. Box 0116, Wuhan 430033, PR China

Received 10 October 2001; received in revised form 21 December 2002

Abstract

In the present investigation on the dynamic plastic buckling of cylindrical shells under axial compression waves, the critical axial stress and the exponential parameter of inertia terms in stability equations are treated as a couple of characteristic parameters. The criterion of transformation and conservation of energy in the process of buckling initiation is used to derive the supplementary restraint equation of buckling deformation at the fronts of axial elastic and plastic compression waves. The supplementary restraint equation, stability equations, boundary conditions and continuity conditions constitute the necessary and sufficient conditions of determining the two characteristic parameters. Two characteristic equations are derived for the two characteristic parameters. The critical axial stress or the critical buckling time, the exponential parameter of inertia terms and the initial modes of buckling deformation are calculated quantitatively from the solution of the characteristic equations.

Keywords: Dynamic buckling; Twin characteristic parameter; Buckling criterion; Cylindrical shell; Elastoplastic wave

1. Introduction

The subject of dynamic buckling of cylindrical shells under axial impulsive loading has been studied by many investigators (Coppa and Nash, 1962; Roth and Klosner, 1964; Budiansky and Hutchinson, 1964; Hutchinson and Budiansky, 1966; Lindberg and Herbert, 1966; Goodier, 1967; Florence and Goodier, 1968; Tamura and Babcock, 1975; Fisher and Bert, 1973; Zimcik and Tennyson, 1980; Lindberg and Florence, 1983; Jones, 1989; Simitses, 1990; Lepik, 1999; Karagiozova and Jonse, 2000). The effect of stress wave propagation and the effect of inertia have important influences on the initiation of dynamic buckling. Some features of dynamic buckling distinct from the corresponding static buckling, for example, the localization of dynamic buckling deformation and the occurrence of higher deformation modes, are related to the effect of stress wave propagation and the effect of inertia. Lepik (1999) investigated the dynamic plastic

* Corresponding author.
E-mail address: wtng4509@public.wh.hb.cn (A. Wang).

0020-7683/03/$ - see front matter © 2003 Elsevier Science Ltd. All rights reserved.
doi:10.1016/S0020-7683(03)00051-9

buckling of cylindrical shells under axial impact by use of quasi-bifurcation method (Lee, 1977), with the effect of stress wave taken into account. In the paper of Karagiozova and Jonse (2000), particular attention was paid to the influence of stress wave propagation on the initiation of buckling by use of the numerical simulation of discrete model.

In the two works done by authors of this paper (Wang and Tian, 2002a,b), attempts were made at determining quantitatively inertial effect in the process of buckling initiation for columns subjected to an axial step-load. The critical axial stress and the exponential parameter of inertia terms in stability equations were treated as a couple of characteristic parameters. The criterion of transformation and conservation of energy in the transient process of buckling was presented to derive the supplementary restraint equation of determining the two characteristic parameters. The method may be known as the twin-characteristic-parameter analysis of dynamic buckling problems.

In this paper, we present the twin-characteristic-parameter analysis of dynamic plastic buckling for cylindrical shells under elastic–plastic compression waves caused by an axial impact. The analysis will be focused on the calculation of the critical axial stress (or critical buckling time), the exponential parameter of inertia, and the initial modes of dynamic buckling deformation. The post-buckling problem is not included in the present analysis.

The analysis is confined to the axisymmetrical deformation modes of cylindrical shells. This restriction is suitable for the cylindrical shell with small radius-to-thickness ratio.

2. Axial compression waves and stability equations for cylindrical shells

As shown in Fig. 1(a), we consider the cylindrical shell of length L^*, radius R and thickness h. It is assumed that the shell is made of linear strain-hardening material with the density ρ. The relation between stress and strain for linear strain-hardening material is shown in Fig. 1(b), where E is Young's modulus and E_t denotes the hardening modulus.

At the instant $t_0 = 0$, an axial compressive force of magnitude N_1 is suddenly applied at the end **A** of the shell, where N_1 denotes the force intensity along the circumference of the shell end. The compressive force may result from axial impact against a rigid wall by the shell with an attached mass or impact against the stationary shell by a traveling mass G. We use σ_1 to denote the axial compressive stress σ_1 caused at the impact end when the impact begins. In this paper, we consider the case where the value of σ_1 is higher than the yield stress of the shell material, that is

$$N_1 = \sigma_1 h, \quad \sigma_1 > \sigma_s \tag{2.1a,b}$$

At the beginning of impact, the elastic compression wave and plastic compression wave resulting from the impact start propagating from the impact end toward the remote end at the velocities c_0 and c_1, respectively.

In this paper, our investigation is confined to the dynamic buckling that occurs at the first two stages of the wave propagation, as shown in the following. In order to avoid the discussion of unloading problem, we assume that the loading duration of the force N_1 is longer than or equal to the period of the two stages.

2.1. Stresses in the unbuckled shell at the first stage of compression-wave propagation

The first stage of compression-wave propagation begins at the instant $t_0 = 0$ when the impact is initiated, and ends at the instant when the elastic wave front arrives at the fixed end for the first time. At this stage, the characteristics representing the position of compression wave fronts and the axial force in the shell are plotted in Fig. 1(c) for the shell made of linear strain-hardening material. At any instant t before the elastic

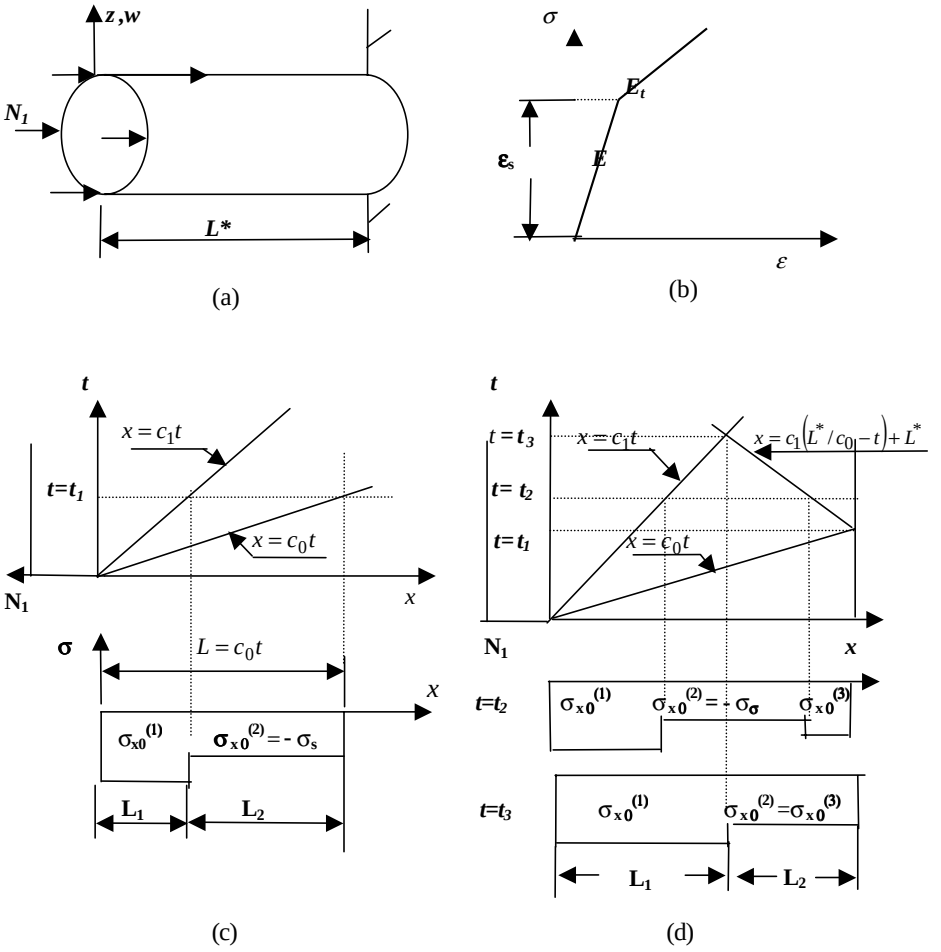

Fig. 1. (a) Cylindrical shell geometry. (b) Relation between stress and strain for linear strain-hardening material. (c) Initial elastic and plastic stress waves in the shell. (d) Initial wave and reflected wave in the shell.

wave front arrives at the fixed end and is reflected, the distances that the elastic and plastic waves travel from the impact end are, respectively,

$$L = c_0 t, \quad L_1 = c_1 t \quad (t \leqslant L^*/c_0) \tag{2.2a, b}$$

The region $0 \leqslant x < L_1$ is the plastic wave region, and the region $L_1 < x \leqslant L$ is the elastic wave region.

For simplicity, we assume that the pre-buckling deformation of the shell may be determined with sufficient accuracy by membrane theory. The stresses in the unbuckled shell are written as

$$\sigma_{x0}^{(1)} = -\sigma_1, \quad \sigma_{x0}^{(2)} = -\sigma_s, \quad \sigma_{\theta 0}^{(1)} = \sigma_{\theta 0}^{(2)} = 0 \tag{2.3a–c}$$

In Eqs. (2.3), the superscripts 1 and 2 are corresponding to the plastic wave region and the elastic wave region, respectively. The force intensities in the unbuckled shell are denoted by $N_{x0}^{(i)}$ and $N_{\theta 0}^{(i)} = 0$ for the two regions. With $u_{x0}^{(i)}$ denoting the axial displacement and $w_0^{(i)}$ denoting the displacement normal to the middle surface, the motion equations of the unbuckled shell are written as

$$E_t u^{(1)}_{x0,xx} = \rho u^{(1)}_{x0,tt} \quad (0 \leqslant x < L_1), \quad E u^{(2)}_{x0,xx} = \rho u^{(2)}_{x0,tt} \quad (L_1 < x < L) \tag{2.4a, b}$$

From the solution of Eqs. (2.4a,b), the values of the elastic wave velocity c_0 and the plastic wave velocity c_1 are calculated. The axial strain of the middle surface of the unbuckled shell is expressed as

$$\varepsilon^{(1)}_{x0} = \left(\frac{1}{E_t} - \frac{1}{E}\right)\sigma_s - \frac{N_1}{E_t h} \quad (0 \leqslant x < L_1), \quad \varepsilon^{(2)}_{x0} = -\frac{\sigma_s}{E} \quad (L_1 < x < L) \tag{2.5a, b}$$

If the amplitude of the stress $\sigma^{(1)}_{x0}$ is large enough, the dynamic buckling of the shell will take place at this stage.

2.2. Stresses in the unbuckled shell at the second stage of compression-wave propagation

The second stage of compression-wave propagation begins at the instant when the elastic wave front arrives at the fixed end and is reflected from the fixed end for the first time. The stage ends at the instant when the reflected wave front meets with the forward plastic wave N_1 . At this stage, the plastic wave has not reached the fixed end. According to the theory of one-dimensional stress waves (Wang Lili, 1985), the stress in the region between the reflected wave front and the reflection end is calculated by use of the following formula:

$$\sigma^{(3)}_{x0} = -\sigma_s\left(1 + \sqrt{E_t/E}\right) \tag{2.6}$$

Consequently, the reflected wave is a plastic compression wave. At this stage, the characteristics representing the position of the fronts of the forward wave and the reflected wave, and the axial force in the shell are plotted in Fig. 1(d). The reflected wave travels towards the impact end at the speed c_1, and meets with the forward plastic wave N_1 at the instant $t = t_3$.

$$t_3 = L(c_0 + c_1)/(2c_0c_1) \tag{2.7}$$

At this stage, we denote the axial length of the shell by L instead of L^*.

2.3. Dynamic-bifurcation equations obtained by use of the adjacent-equilibrium criterion

We assume that the buckling occurs with axisymmetric deformation modes for the shell under the action of elastic and plastic compression waves. At the initial stage of buckling occurrence, the displacements of the middle surface have the infinitesimal increments $(u^{(1)}_{x1}, w^{(1)}_1)$ for the region $0 \leqslant x < L_1$ and $(u^{(2)}_{x1}, w^{(2)}_1)$ for the region $L_1 < x < L$. Corresponding to the displacement increments $u^{(i)}_{x1}$ and $w^{(i)}_1$, the increments of the in-plane forces are $N^{(i)}_{x1}$ and $N^{(i)}_{\theta 1}$, and the moment intensity on circumferential cross-section is denoted by M_x. After buckling, the total displacements are written as

$$u^{(i)}_x = u^{(i)}_{x0} + u^{(i)}_{x1}, \quad w^{(i)} = w^{(i)}_0 + w^{(i)}_1, \qquad i = 1, 2 \tag{2.8a, b}$$

The displacements $(u^{(i)}_{x0}, w^{(i)}_0)$ and $(u^{(i)}_x, w^{(i)})$ correspond to two adjacent-equilibrium configurations. From the theory of thick shells (Tessler et al., 1995) we derive the following governing equations for the axisymmetric dynamic buckling by use of the adjacent-equilibrium criterion similar to that in the static instability theory (Brush and Almroth, 1975).

$$\begin{aligned} N^{(i)}_{x1,x} &= \rho h\left(u^{(i)}_{x1,tt} + \frac{1}{12}\frac{h^2}{R}\theta_{1,tt}\right), \quad M^{(i)}_{x,xx} + \left(N^{(i)}_{x0} w^{(i)}_{1,x}\right)_{,x} - \frac{N^{(i)}_{\theta 1}}{R} \\ &= \rho h\left(w^{(i)}_{1,tt} + \frac{1}{12}\frac{h^2}{R}u_{x1,xtt} + \frac{1}{12}h^2\theta_{1,xtt}\right), \qquad i = 1, 2 \end{aligned} \tag{2.9a, b}$$

In Eqs. (2.9a,b), θ_1 denotes the cross-section rotation in the axial direction. For simplification, let us estimate the magnitude order of the terms at the right side of Eqs. (2.9a,b).

$$\theta_1 = \mathrm{O}(w_{1,x}), \quad \frac{1}{12}\frac{h^2}{R}\theta_{1,tt} = \mathrm{O}\left(\frac{1}{12}\frac{h^2}{lR}w_{1,tt}\right), \quad \frac{1}{12}\frac{h^2}{R}u_{x1,xtt} = \mathrm{O}\left(\frac{1}{12}\frac{h^2}{lR}u_{x1,tt}\right),$$
$$\frac{1}{12}h^2\theta_{1,xtt} = \mathrm{O}\left(\frac{h^2}{12l^2}w_{1,tt}\right) \tag{2.10a–d}$$

In Eqs. (2.10a–d), l denotes the variation length of the variables u_1 and w_1 along the axial direction of the shell, and is half as large as the length of buckling half-wave. From the numerical results of calculation, the variation length l is approximately of the same order of magnitude as the radius R. At the right side of Eq. (2.9b), the ratio of the second or third term to the first term is of the magnitude order $h^2/(12R^2)$, approximately. Therefore, the second and third terms may be omitted in comparison with the first term in the following analysis. For the same reason, the second term at the right side of Eq. (2.9a) is also omitted. With the above-mentioned simplification, Eqs. (2.9a,b) are rewritten as

$$N^{(i)}_{x1,x} = \rho h u^{(i)}_{x1,tt}, \quad M^{(i)}_{x,xx} + \left(N^{(i)}_{x0}w^{(i)}_{1,x}\right)_{,x} - \frac{N^{(i)}_{\theta 1}}{R} = \rho h w^{(i)}_{1,tt}, \qquad i = 1,2 \tag{2.11a, b}$$

3. Fundamental equations derived by use of deformation theory

In the following, we will transform Eq. (2.11) into the form expressed by the buckling displacements $w^{(i)}_1$ and $u^{(i)}_1$ according to the deformation theory of plasticity.

Assuming that the cross-section of the shell remains plane at the initial stage of buckling deformation, we write the expressions of the strain increments $e^{(i)}_{x1}$ and $e^{(i)}_{\theta 1}$ as follows:

$$e^{(i)}_{x1} = \varepsilon^{(i)}_{x1} - z w^{(i)}_{1,xx}, \quad \varepsilon^{(i)}_{x1} = u^{(i)}_{1,x}, \quad e^{(i)}_{\theta 1} = \varepsilon^{(i)}_{\theta 1} = \frac{w^{(i)}_1}{R+z} \tag{3.1a–c}$$

where $\varepsilon^{(i)}_{x1}$ and $\varepsilon^{(i)}_{\theta 1}$ represent the buckling strains of the middle surface.

We assume that no strain-rate reversal occurs at the initial stage of buckling deformation. Under this assumption, there is no unloading zone in the shell. The relations between the stress increments and the strain increments derived by use of deformation theory of plasticity (Wang Ren et al., 1998) are written as follows:

$$\sigma^{(i)}_{x1} = \left(E_t + \frac{E^{(i)}_s}{3}\right)e^{(i)}_{x1} + \frac{2E^{(i)}_s}{3}e^{(i)}_{\theta 1}, \quad \sigma^{(i)}_{\theta 1} = \frac{4E^{(i)}_s}{3}\left(e^{(i)}_{\theta 1} + \frac{1}{2}e^{(i)}_{x1}\right) \tag{3.2a, b}$$

In Eqs. (3.2a,b), $E^{(i)}_s$ denotes the secant modulus and is calculated according to the following equation:

$$\frac{1}{E^{(i)}_s} = \frac{1}{E_t} - \left(\frac{1}{E_t} - \frac{1}{E}\right)\frac{\sigma_s h}{N_i} \tag{3.3}$$

By integration, we obtain

$$M^{(i)}_x = \int_{-h/2}^{h/2}\sigma^{(i)}_{x1}\left(1+\frac{z}{R}\right)z\,\mathrm{d}z \approx -\frac{h^3}{12}\left(E_t + \frac{E^{(i)}_s}{3}\right)w^{(i)}_{1,xx} \tag{3.4}$$

$$N^{(i)}_{x1} = \int_{-h/2}^{h/2}\sigma^{(i)}_{x1}\left(1+\frac{z}{R}\right)\mathrm{d}z \approx \left(E_t + \frac{E^{(i)}_s}{3}\right)h u^{(i)}_{1,x} + \frac{2}{3}E^{(i)}_s h\frac{w^{(i)}_1}{R} \tag{3.5}$$

$$N_{\theta 1}^{(i)} = \int_{-h/2}^{h/2} \sigma_{\theta 1}^{(i)} \, \mathrm{d}z \approx \frac{4}{3} E_{\mathrm{s}}^{(i)} h \left(\frac{w_1^{(i)}}{R} + \frac{1}{2} u_{1,x}^{(i)} \right) \tag{3.6}$$

Introducing Eq. (3.5) into Eq. (2.11a) gives

$$\left(E_t + \frac{E_{\mathrm{s}}^{(i)}}{3} \right) u_{1,xx}^{(i)} + \frac{2E_{\mathrm{s}}^{(i)}}{3R} w_{1,x}^{(i)} = \rho u_{1,tt}^{(i)} \tag{3.7}$$

In the axial direction, the following boundary conditions and continuity conditions are employed for the shell impacted against a rigid wall.

$$u_1^{(1)}(0,t) = 0, \quad N_{x1}^{(2)}(L,t) = 0, \tag{3.8a, b}$$

$$u_1^{(1)}(c_1 t, t) = u_1^{(2)}(c_1 t, t), \quad N_{x1}^{(1)}(c_1 t, t) = N_{x1}^{(2)}(c_1 t, t) \tag{3.9a, b}$$

From the numerical results of investigation on dynamic elastic buckling (Wang and Tian, 2002a,b), it has been found that the influence of the axial inertia effect is small. With omitting the axial inertia term at the right side of Eq. (3.7), by integration we obtain

$$u_{1,x}^{(i)} = -\frac{2E_{\mathrm{s}}^{(i)}}{E_{\mathrm{s}}^{(i)} + 3E_t} \frac{w_1^{(i)}}{R} \tag{3.10}$$

With introducing Eqs. (3.4), (3.6) and (3.10), we re-write Eq. (2.11b) as

$$D_{\mathrm{s}}^{(i)} w_{1,xxxx}^{(i)} + N_i w_{1,xx}^{(i)} + \frac{C_i}{R^2} w_1^{(i)} + \rho h w_{1,tt}^{(i)} = 0 \tag{3.11}$$

$$D_{\mathrm{s}}^{(i)} = \frac{h^3}{12} \left(E_t + \frac{E_{\mathrm{s}}^{(i)}}{3} \right), \quad C_i = \frac{4E_t h}{1 + 3E_t / E_{\mathrm{s}}^{(i)}} \tag{3.12a, b}$$

In this paper, we consider two types of radial boundary conditions at the shell ends. The first type of radial boundary conditions is assumed to be that transverse force and cross-section rotation at one end or both ends of the shell are equal to zero, and is written as follows:

$$w_{1,x}^{(i)} = 0, \quad D w_{1,xxx}^{(i)} + N_i w_{1,x}^{(i)} = 0 \tag{3.13a, b}$$

For the second type of radial boundary conditions, we assume that the shell is simply supported at one end or both ends. The boundary conditions are written as

$$w_1^{(i)} = 0, \quad w_{1,xx}^{(i)} = 0 \tag{3.14a, b}$$

When the dynamic buckling occurs at the first stage of the compression-wave propagation, the portion of the shell before the front of the elastic compression wave remains undisturbed. The restraint conditions at the elastic wave front $x^* = c_0 t$ are written as

$$w_1^{(2)}(c_0 t, t) = 0, \quad w_{1,x}^{(2)}(c_0 t, t) = 0 \tag{3.15a, b}$$

The continuity conditions at the front of the plastic compression wave are written in the forms:

$$\begin{aligned} &w_1^{(1)}(c_1 t, t) = w_1^{(2)}(c_1 t, t), \quad w_{1,x}^{(1)}(c_1 t, t) = w_{1,x}^{(2)}(c_1 t, t), \\ &D_{\mathrm{s}}^{(1)} w_{1,xx}^{(1)}(c_1 t, t) = D_{\mathrm{s}}^{(2)} w_{1,xx}^{(2)}(c_1 t, t), \\ &D_{\mathrm{s}}^{(1)} w_{1,xxx}^{(1)}(c_1 t, t) + N_1 w_{1,x}^{(1)}(c_1 t, t) = D_{\mathrm{s}}^{(2)} w_{1,xxx}^{(2)}(c_1 t, t) + N_2 w_{1,x}^{(2)}(c_1 t, t) \end{aligned} \tag{3.16a–d}$$

4. Transformation and conservation of energy in process of buckling and supplementary restraint equation at compression wave fronts

We write Eq. (3.11) into the form:

$$w^{(i)}_{1,xxxx} + \alpha_i^2 w^{(i)}_{1,xx} + \psi_i^2 w^{(i)}_1 + \gamma_i^2 w^{(i)}_{1,tt} = 0 \tag{4.1}$$

In Eq. (4.1), the parameters α_i, ψ_i and γ_i are respectively defined as

$$\alpha_i^2 = \frac{N_i}{D_s^{(i)}}, \quad \psi_i^2 = \frac{C_i}{D_s^{(i)} R^2}, \quad \gamma_i^2 = \frac{\rho h}{D_s^{(i)}} \tag{4.2a–c}$$

In many cases for dynamically loaded cylindrical shells, experimental results have shown that at the initial stage of buckling occurrence, the waveform remains in a fixed position and merely grows in amplitude with time (Lindberg and Florence, 1983). For this reason, the buckling displacement $w_1^{(i)}$ may be written into the variable-separated form as follows:

$$w_1^{(i)}(x,t) = T(t) Y_i(x) \tag{4.3}$$

Substituting Eq. (4.3) into Eq. (4.1), we obtain the following equations:

$$\ddot{T} - \lambda T = 0, \quad Y_i''''(x) + \alpha_i^2 Y_i''(x) + \tilde{\omega}_i^2 Y_i(x) = 0, \quad \tilde{\omega}_i^2 = \psi_i^2 + \gamma_i^2 \lambda, \qquad i = 1,2 \tag{4.4a–c}$$

In Eqs. (4.4), dots and primes denote differentiation with respect to the time variable t and the axial coordinate x respectively, and λ is the undetermined parameter that is named the inertial characteristic parameter.

When the dynamic buckling occurs, the buckling deflection $w_1^{(i)}$ increases with the time variable t. In this case, for the solution of Eq. (4.4a) we have

$$\lambda = \omega^2 > 0, \quad T = b\mathrm{e}^{\omega(t-t_{\mathrm{cr}})} \tag{4.5a, b}$$

In Eq. (4.5b), t_{cr} denotes the critical buckling time and b is an infinitesimal integration constant.

For the problem under consideration, there are two characteristic parameters α_1 and $\omega = \sqrt{\lambda}$ that need to be determined. For the two parameters, only one characteristic equation is derived from the condition on which the governing equation (4.4b) has a nontrivial solution satisfying the boundary conditions (3.13)–(3.15) and the continuity conditions Eq. (3.16). We have to find the supplementary condition of determining the two characteristic parameters.

We introduce the following denotations:

$$x^{(1)}_{\mathrm{lo}} = 0, \quad x^{(1)}_{\mathrm{up}} = x^{(2)}_{\mathrm{lo}} = c_1 t, \quad L^{(2)}_{\mathrm{up}} = c_0 t \tag{4.6a–c}$$

With multiplying both sides of Eqs. (2.11b) by $w_1^{(i)}$ and integrating it by parts, we derive the following equation:

$$\begin{aligned} &\sum_{i=1}^{2} \int_{x^{(i)}_{\mathrm{lo}}}^{x^{(i)}_{\mathrm{up}}} \left[M^{(i)}_{x,xx} + \left(N^{(i)}_{x0} w^{(i)}_{1,x} \right)_{,x} - \frac{N^{(i)}_{\theta 1}}{R} - \rho h w^{(i)}_{1,tt} \right] w^{(i)}_1 \, \mathrm{d}x \\ &\quad = \sum_{i=1}^{2} \left\{ \int_{x^{(i)}_{\mathrm{lo}}}^{x^{(i)}_{\mathrm{up}}} M^{(i)}_x w^{(i)}_{1,xx} \, \mathrm{d}x + \int_{x^{(i)}_{\mathrm{lo}}}^{x^{(i)}_{\mathrm{up}}} N_i \left(w^{(i)}_{1,x} \right)^2 \mathrm{d}x - \int_{x^{(i)}_{\mathrm{lo}}}^{x^{(i)}_{\mathrm{up}}} N^{(i)}_{\theta 1} \varepsilon^{(i)}_{\theta 1} \, \mathrm{d}x - \rho h \int_{x^{(i)}_{\mathrm{lo}}}^{x^{(i)}_{\mathrm{up}}} \left(w^{(i)}_{1,t} \right)^2 \mathrm{d}x \right\} = 0 \end{aligned} \tag{4.7}$$

We introduce the following expressions:

$$U_{\mathrm{rel}} = \sum_{i=1}^{2}\left(\frac{1}{2}\int_{x_{\mathrm{lo}}^{(i)}}^{x_{\mathrm{up}}^{(i)}} N_i\left(w_{1,x}^{(i)}\right)^2 \mathrm{d}x\right)$$
$$U_{\mathrm{buc}} = \sum_{i=1}^{2}\frac{1}{2}\left(\int_{x_{\mathrm{lo}}^{(i)}}^{x_{\mathrm{up}}^{(i)}} N_{\theta 1}^{(i)}\varepsilon_{\theta 1}^{(i)}\,\mathrm{d}x - \int_{x_{\mathrm{lo}}^{(i)}}^{x_{\mathrm{up}}^{(i)}} M_x^{(i)} w_{1,xx}^{(i)}\,\mathrm{d}x\right) \tag{4.8a–c}$$
$$K_w = \sum_{i=1}^{2}\left(\frac{1}{2}\rho h\int_{x_{\mathrm{lo}}^{(i)}}^{x_{\mathrm{up}}^{(i)}} (w_{1,t}^{(i)})^2\,\mathrm{d}x\right)$$

The axial strain corresponding to the buckling deflection $w_1^{(i)}$ is

$$\tilde{\varepsilon}_{x1}^{(i)} = \frac{1}{2}w_{x1,x}^{(i)} \tag{4.9}$$

With the expressions (4.8a–c) introduced, Eq. (4.7) is written as

$$U_{\mathrm{rel}} = U_{\mathrm{buc}} + K_w \tag{4.10}$$

In Eqs. (4.8a–c), U_{rel} represents the decreased compressive-deformation energy in the shell, related to the buckling displacement $w_1^{(i)}$, U_{buc} denotes the buckling deformation energy and K_w is the buckling kinetic energy corresponding to the velocity $\dot{w}_1^{(i)}$. Eq. (4.10) expresses the transformation and conservation of energy in the transient process of buckling initiation, and may be used as the critical condition of dynamic buckling.

Differentiating both sides of Eq. (4.10) with respect to the time variable t, we obtain the second critical condition of dynamic buckling:

$$\dot{U}_{\mathrm{rel}} = \dot{U}_{\mathrm{buc}} + \dot{K}_w \tag{4.11}$$

Eq. (4.11) may be interpreted as the conservation of the energy transformation rate in the process of the dynamic buckling. The critical condition (4.10) and (4.11) constitute the criterion of the dynamic instability for the cylindrical shell under the action of axial compressive waves.

For the dynamic buckling caused by the axial compression wave traveling at the first stage as shown in Fig. 1(c), introducing Eqs. (4.8a–c) into Eq. (4.11) gives the following supplementary restraint equation of buckling deformations at the fronts of compression waves:

$$Y_2''(c_0 t) = \pm\sqrt{\frac{c_1(N_1 - N_2)}{c_0 D_{\mathrm{s}}^{(2)}}}\,Y_2'(c_1 t) \tag{4.12}$$

The selection of the signs '±' at the right side of Eq. (4.12) should ensure that the values of both sides of the equation have the same sign.

For the dynamic buckling at the instant $t = t_3$ when the forward plastic wave meets the reflected plastic wave, as shown in Fig. 1(d), the supplementary restraint equation obtained from the critical condition (4.11) is

$$Y_1'(c_1 t_3) = Y_2'(c_1 t_3) = 0 \tag{4.13}$$

Eq. (4.4b), the boundary conditions (3.13)–(3.15), the continuity conditions (3.16) and the supplementary restraint equation (4.12) or (4.13) constitute the necessary and sufficient conditions of determining the solution of the buckling problem.

5. Solution for two characteristic parameters and buckling modes

5.1. Solutions of Eq. (4.4b) for buckling at the first stage of compression-wave propagation

For the dynamic buckling at the first stage of compression-wave propagation as shown in Fig. 1(c), the conditions of determining the solution of Eq. (4.4b) consist of the boundary conditions (3.13) or (3.14) at the impact end, the restraint conditions (3.15) at the elastic wave front, the continuity conditions (3.16) at the front of plastic wave, and the supplementary restraint equation (4.12). By investigation, it is found that only for the case $\alpha_1^2 > 2\tilde{\omega}_1$ and $2\tilde{\omega}_2 > \alpha_2^2$, Eq. (4.4b) have the nontrivial solution satisfying the restraint conditions as mentioned above. The expressions of the solution are written in the following forms:

$$Y_1(x) = D_1\cos(\beta_1 x) + D_2\sin(\beta_1 x) + D_3\cos(\beta_2 x) + D_4\sin(\beta_2 x) \tag{5.1}$$

$$Y_2(x) = ch(\zeta_1 x)[d_1\cos(\zeta_2 x) + d_2\sin(\zeta_2 x)] + sh(\zeta_1 x)[d_3\cos(\zeta_2 x) + d_4\sin(\zeta_2 x)] \tag{5.2}$$

In Eqs. (5.1) and (5.2), D_i and d_i ($i = 1, 2, 3, 4$) are integration constants. The parameters β_i and ς_i ($i = 1, 2$) are defined as

$$\beta_1 = \sqrt{\frac{1}{2}\left[\alpha_1^2 + \sqrt{\alpha_1^4 - 4\tilde{\omega}_1^2}\right]}, \quad \beta_2 = \sqrt{\frac{1}{2}\left[\alpha_1^2 - \sqrt{\alpha_1^4 - 4\tilde{\omega}_1^2}\right]} \tag{5.3a, b}$$

$$\alpha_1^2 = \beta_1^2 + \beta_2^2, \quad \tilde{\omega}_1 = \sqrt{\psi_1^2 + \gamma_1^2\lambda} = \beta_1\beta_2 \tag{5.4a, b}$$

$$\zeta_1 = \frac{1}{2}\sqrt{2\tilde{\omega}_2 - \alpha_2^2}, \quad \zeta_2 = \frac{1}{2}\sqrt{2\tilde{\omega}_2 + \alpha_2^2}, \quad \gamma_1^2(\tilde{\omega}_2^2 - \psi_2^2) = \gamma_2^2(\tilde{\omega}_1^2 - \psi_1^2) \tag{5.5a, b, c}$$

From Eq. (5.4b), the expression of the inertial exponential parameter ω is written as

$$\frac{\omega}{c_0 h} = \sqrt{\frac{1}{12}\left(\frac{E_t}{E} + \frac{E_s^{(1)}}{3E}\right)\left(\tilde{\omega}_1^2 - \psi_1^2\right)} \tag{5.6}$$

5.2. Solutions of Eq. (4.4b) for buckling at the second stage of compression-wave propagation

At the instant $t = t_3$, as shown in Fig. 1(d), the plastic wave traveling forward from the impact end meets the reflected plastic wave traveling backward from the reflecting end. For the dynamic buckling occurring at the instant $t = t_3$, the conditions of determining the solution of Eq. (4.4b) consist of the boundary conditions (3.13) or (3.14) at both ends of the shell, the continuity conditions (3.16) and the supplementary restraint condition (4.13) at the plastic wave front.

For Eqs. (4.4b), the expression of the solution $Y_1(x)$ is the same as Eq. (5.1), and $Y_2(x)$ is of the same form as $Y_1(x)$ and written as

$$Y_2(x) = d_1\cos(\xi_1 x) + d_2\sin(\xi_1 x) + d_3\cos(\xi_2 x) + d_4\sin(\xi_2 x) \tag{5.7}$$

$$\xi_1 = \sqrt{\frac{1}{2}\left[\alpha_2^2 + \sqrt{\alpha_2^4 - 4\tilde{\omega}_2^2}\right]}, \quad \xi_2 = \sqrt{\frac{1}{2}\left[\alpha_2^2 - \sqrt{\alpha_2^4 - 4\tilde{\omega}_2^2}\right]} \tag{5.8a, b}$$

$$\alpha_2^2 = \xi_1^2 + \xi_2^2, \quad \tilde{\omega}_2 = \xi_1\xi_2 \tag{5.9a, b}$$

5.3. Equations for the two characteristic parameters

Introducing the expressions (5.1) and (5.2) or the expressions (5.1) and (5.7) into the boundary conditions, continuity conditions and supplementary restraint equation as mentioned above, we obtain nine linear algebraic equations for the eight constants D_i and d_i ($i = 1, 2, 3, 4$). From the conditions of the existence of nontrivial solution for these equations, we derive the two characteristic equations for the parameters β_1 and β_2 as follows:

$$F_1(\beta_1, \beta_2, k, \eta) = 0, \quad F_2(\beta_1, \beta_2, k, \eta) = 0 \tag{5.10a, b}$$

where the parameters β_1 and β_2 are related to the characteristic parameters α_1^2 and $\omega = \sqrt{\lambda}$ according to Eqs. (5.3a,b) and (5.6). The parameters k and η are defined as

$$k = \sigma_{x0}^{(1)}/\sigma_{x0}^{(2)}, \quad \eta = c_1 t/(L - c_1 t) \tag{5.11a, b}$$

After the values of the parameters β_1 and β_2 are obtained from Eqs. (5.10a,b), the critical-load parameter α_1^2 and the inertial characteristic parameter λ or ω are calculated by use of Eqs. (5.4a,b) and (5.6). Dynamic buckling modes are calculated by use of Eqs. (5.1) and (5.2) or (5.7).

6. Numerical results

By use of the theoretical method developed in Sections 1–5, we have investigated the axisymmetric dynamic plastic buckling of three specimens in the experimental investigation reported by Florence and Goodier (1968), which were investigated by Lepik (1999). In the experiment, specimens attached a large rigid mass at one end were impacted against a rigid wall at another end. The serial numbers of the three specimens are 1, 17 and 23 respectively, in the paper of Florence and Goodier (1968).

The specimens were made of aluminum-alloy 6061-T6. In our calculation, the elastic and hardening moduli of the specimen material are taken as $E = 68.5$ GPa and $E_t = 0.02E$ respectively, which are the same as those in the paper of Lepik (1999). The yield stress of the material is taken as $\sigma_s = 290$ MPa, which is approximately equal to the mean value of the yield stresses given in the papers of Florence and Goodier (1968) and Lepik (1999). The geometrical parameters and experimental impact velocities of the three specimens, given in the paper of Florence and Goodier (1968), are listed in Table 1.

6.1. Dynamic buckling at the first stage of compression-wave propagation

The first stage of axial-compression-wave propagation in shells has been defined in Section 2.1, as shown in Fig. 1(c). From calculation, it is found that the initial buckling deformation occurs at this stage when the impact velocities are equal to the values given in Table 1.

In calculation, we consider the two types of boundary conditions at the impact end, which are defined by Eqs. (3.13a,b) and (3.14a,b) respectively. The boundary conditions Eq. (3.13a,b) are corresponding to the case of zero rotation and zero transverse force at the impact end, that is, the case where in the process of

Table 1
Geometrical sizes and experimental impact velocities for the three models in the paper of Florence and Goodier (1968)

Model no.	Thickness h (in.)	Radius R (in.)	Length L (in.)	Experimental impact velocity v_0 (ft/s)
1	0.095	0.5	3	332
17	0.100	0.5	4	395
23	0.095	0.5	6	310

impact, the shell's edge remains normal to the rigid wall and there is no friction between the rigid wall and the impact end of the shell. In the following, the boundary conditions (3.13a,b) are simply written as ZRZF boundary. At the first stage of wave propagation, Eqs. (3.14a,b) denotes the boundary conditions of simple support at the impact end, which is simply written as SS boundary.

For the boundary ZRZF, two types of buckling deformation modes are obtained from calculation. With the impact velocities given in Table 1, the two types of buckling modes for the specimens 1 and 17 are plotted in Figs. 2–5. In Figs. 2–5, t_{cr} denotes the critical buckling time, and $L_{cr} = c_0 t_{cr}$ denotes the distance that the elastic compression wave travels from the impact end at the instant $t = t_{cr}$. In the figures, σ_1 denotes the axial compression stress in the plastic wave region and σ_s is the yield stress. Corresponding to the impact velocities given in Table 1, the values of the ratio σ_1/σ_s are respectively 1.694, 1.825 and 1.620 for the specimens 1, 17 and 23. Assuming that the buckling occurs at the instant $t = t_1 = L/c_0$, the first type of buckling modes for the specimens 17 and 23 are plotted in Figs. 6 and 7, respectively. For this case, the critical length L_{cr} is equal to the axial length of the shell. For the buckling at this instant, the values of the ratio σ_1/σ_s are calculated and given in the figures, and the axial half-wave numbers of the buckling modes are 8, 11 and 16 for the three specimens, respectively.

The variation of the critical buckling time t_{cr} with the values of the ratio σ_1/σ_s is illustrated in Figs. 8 and 9 for the two types of buckling modes. From Figs. 8 and 9, it is obvious that the critical buckling time t_{cr}

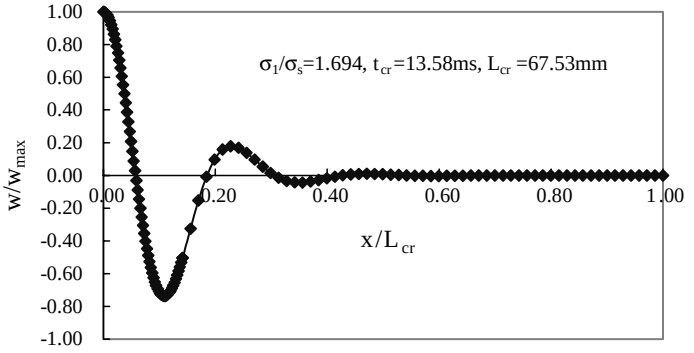

Fig. 2. The first mode of the specimen 1 at the first stage for the boundary condition of zero rotation and zero transverse force at the impact end.

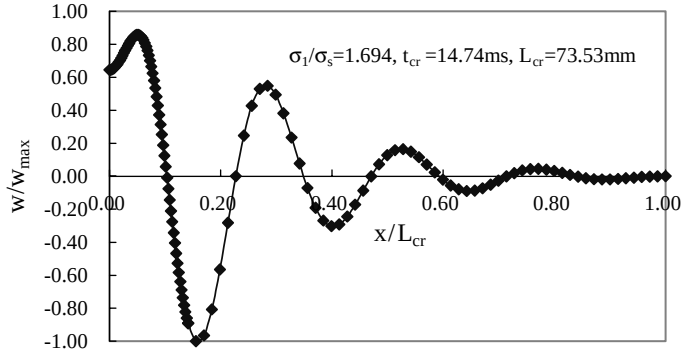

Fig. 3. The second mode of the specimen 1 at the first stage for the boundary condition of zero rotation and zero transverse force at the impact end.

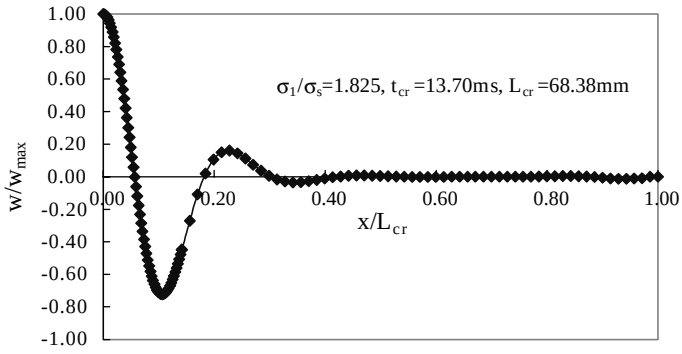

Fig. 4. The first mode of the specimen 17 at the first stage for the boundary condition of zero rotation and zero transverse force at the impact end.

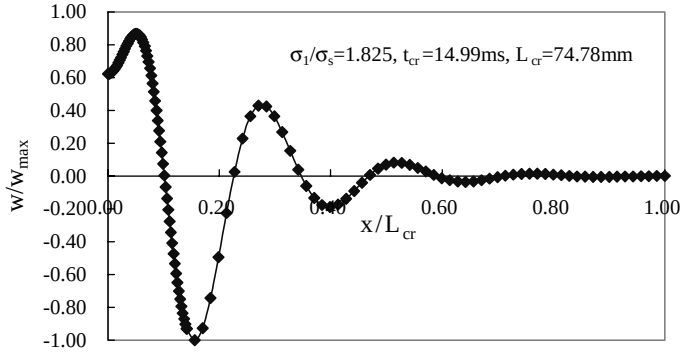

Fig. 5. The second mode of the specimen 17 at the first stage for the boundary condition of zero rotation and zero transverse force at the impact end.

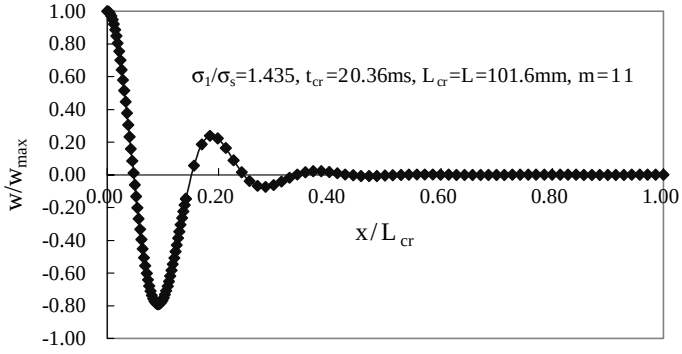

Fig. 6. The first mode of specimen 17 for the boundary condition of zero rotation and zero transverse force at the impact end when buckling occurs at the final instant of the first stage.

decreases with the increment of the stress ratio σ_1/σ_s. The critical buckling time corresponding to the second mode is longer than that for the first mode. Therefore, the dynamic buckling will occur with the first

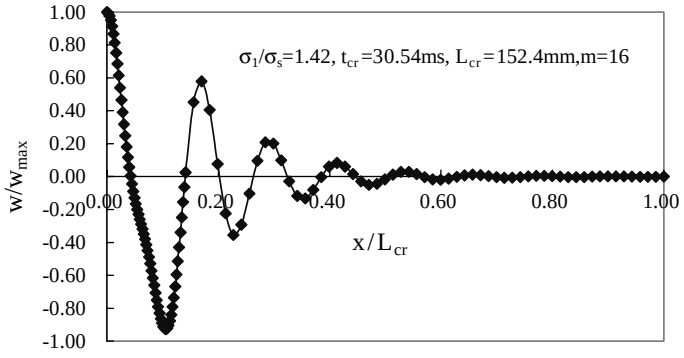

Fig. 7. The first mode of specimen 23 for the boundary condition of zero rotation and zero transverse force at the impact end when buckling occurs at the final instant of the first stage.

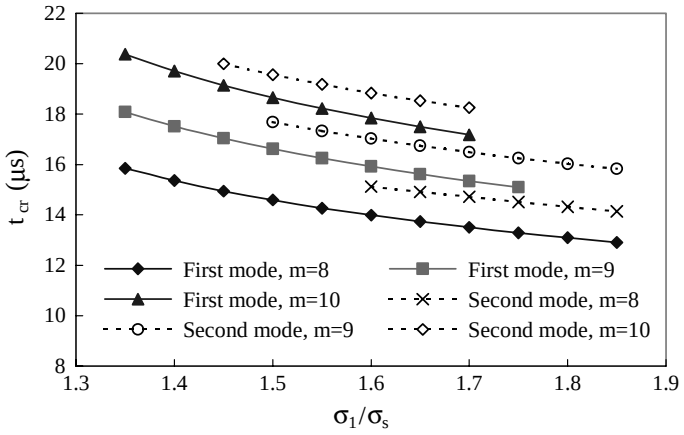

Fig. 8. Critical buckling time t_{cr} of the cylindrical shell at the first stage for ZRZF boundary condition at the impact end. The parameters of shell: $d = 25.4$ mm, $h = 2.41$ mm.

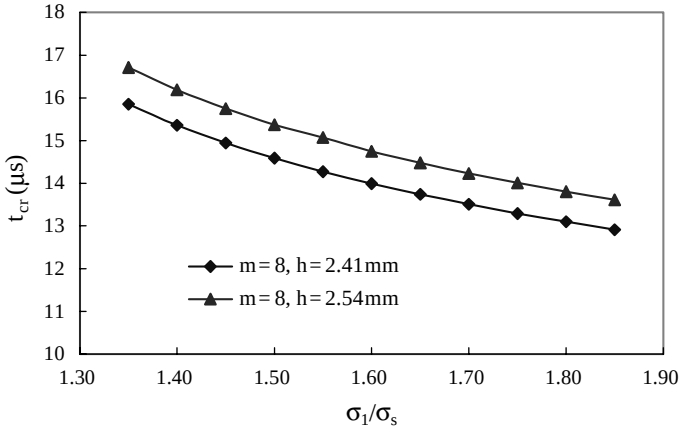

Fig. 9. Critical buckling time t_{cr} of the cylindrical shell corresponding to the first type of modes for ZRZF boundary condition at the impact end ($d = 25.4$ mm).

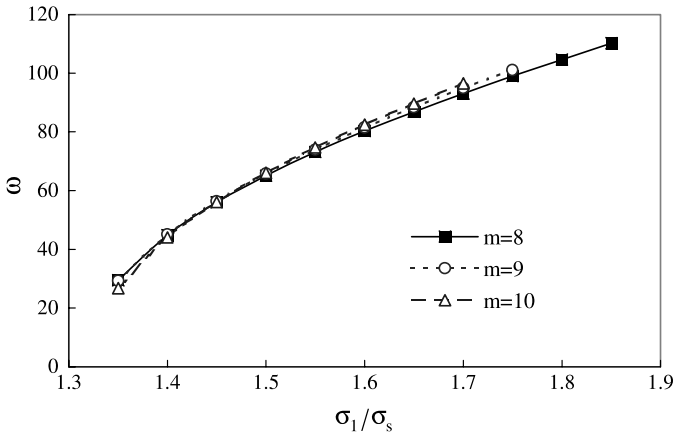

Fig. 10. The value of characteristic parameter ω corresponding to the first buckling mode under the boundary condition of zero rotation and zero transverse force at the impact end ($h = 2.41$ mm).

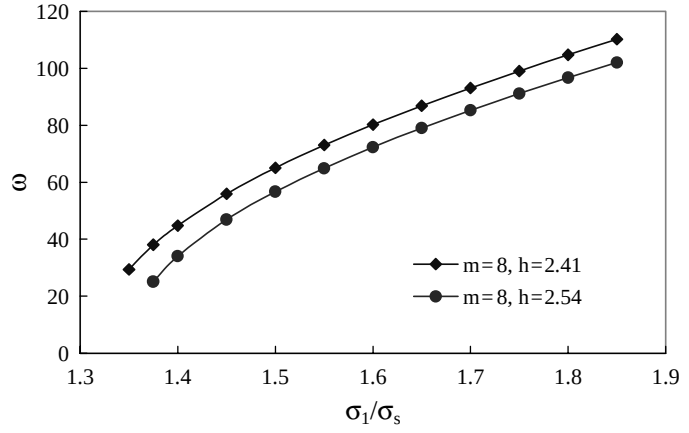

Fig. 11. The value of characteristic parameter ω corresponding to the first buckling mode under the boundary conditions of zero rotation and zero transverse force at the impact end, for different thickness of shells.

mode. The variation of the values of the inertial exponential parameter ω with ratio σ_1/σ_s is illustrated in Figs. 10 and 11 for the first type of buckling modes. From Figs. 10 and 11, it can be seen that the value of the parameter ω increases with the increment of the stress ratio σ_1/σ_s.

For the boundary conditions of simple support (SS) at the impact end, the two types of buckling modes are also obtained from calculation. Corresponding to the impact velocities given in Table 1, the two types of buckling modes for the specimens 1 are plotted in Figs. 12 and 13. For the buckling that occurs at the instant $t = t_1 = L/c_0$, the axial half-wave numbers of the buckling modes are given in Table 2 for the three specimens, and the first type of buckling modes for the specimens 17 and 23 is shown in Figs. 14 and 15, respectively. The variation of the critical buckling time t_{cr} with the ratio σ_1/σ_s is shown in Fig. 16. The variation of the inertial exponential parameter ω with ratio σ_1/σ_s is plotted in Fig. 17. The comparisons of the critical buckling time and the inertial exponential parameter corresponding to the two types of boundary conditions are also give in Figs. 16 and 17. From Fig. 16, it can be seen that the values of the critical buckling time t_{cr} are close to each other for the two types of boundary conditions. The axial half-

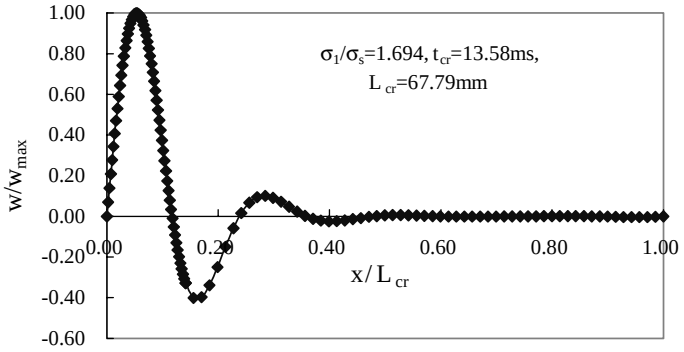

Fig. 12. The first mode of the specimen 1 at the first stage for the boundary conditions of simple support at the impact end.

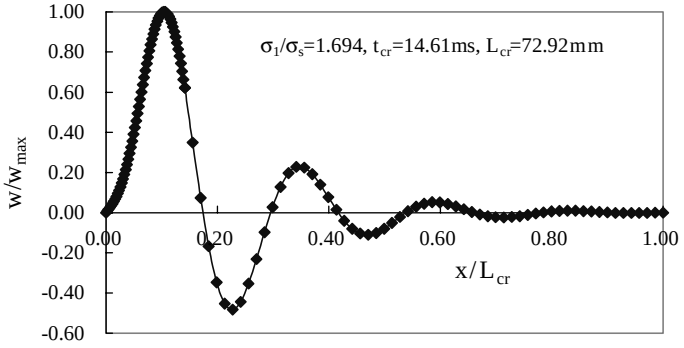

Fig. 13. The second mode of the specimen 1 at the first stage for the boundary conditions of simple support at the impact end.

Table 2
The comparison of axial buckling half-wave numbers m for the three specimens

Model no.	Experiment[a]	The present solution				Solution of Florence and Goodier (1968)	Solution of Lepik (1999)
		Buckling at instant $t = t_1$		Buckling at instant $t = t_3$			
		ZRZF boundary	SS boundary	ZRZF boundary	SS boundary		
1	8	8	8	8	8	10	10
17	11	11	11	11	13	13	13
23	15	16	16	15	18	21	19

[a] The experimental results from the paper of Florence and Goodier (1968).

wave numbers of the buckling modes for the SS boundary conditions are the same as those for the ZRZF boundary conditions.

6.2. Dynamic buckling at the second stage of compression-wave propagation

The second stage of the compression-wave propagation has been defined in Section 2.2. For this stage of the compression-wave propagation, by use of the solution developed in Sections 1–5 we investigate the

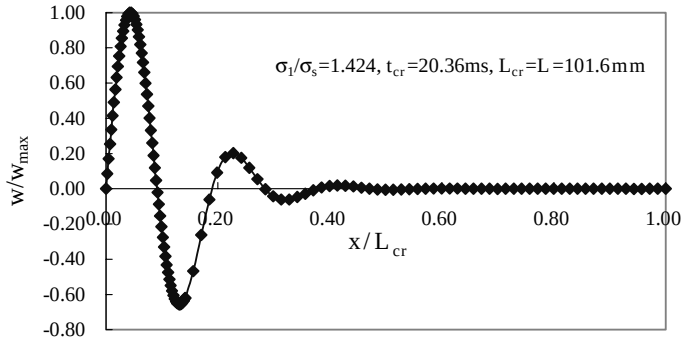

Fig. 14. The first mode of the specimen 17 for the boundary conditions of simple support at the impact end when buckling occurs at the final instant of the first stage.

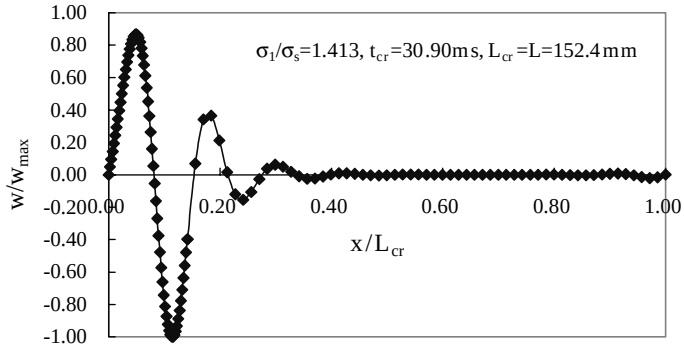

Fig. 15. The first mode of the specimen 23 for the boundary conditions of simple support at the impact end when buckling occurs at the final instant of the first stage.

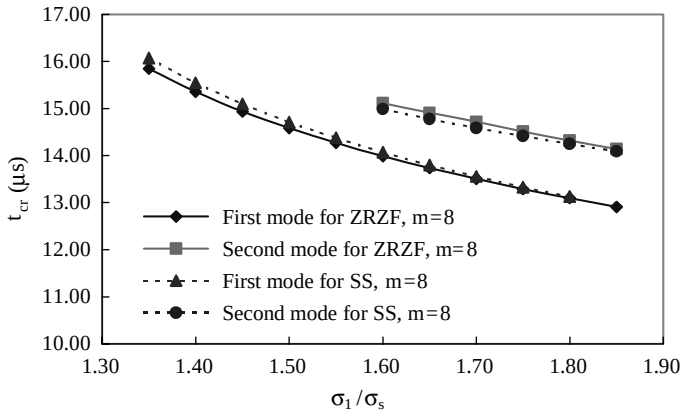

Fig. 16. Comparison of Critical buckling times t_{cr} for ZRZF and SS boundary conditions at the impact end ($h = 2.41$ mm).

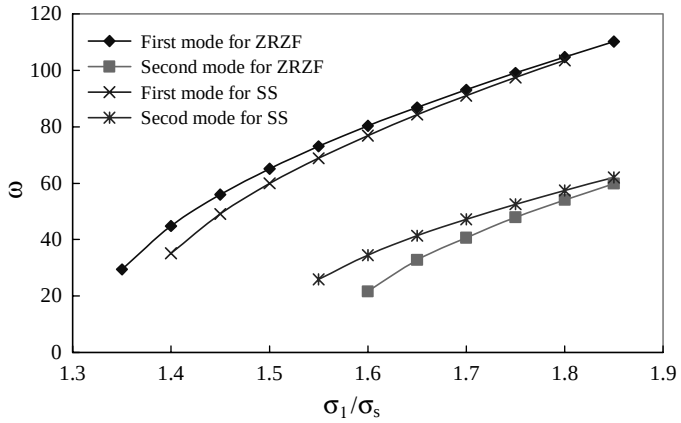

Fig. 17. The comparison of the characteristic parameter ω corresponding to the half-wave number $m = 8$, for the two types of boundary conditions at the impact end ($h = 2.41$ mm).

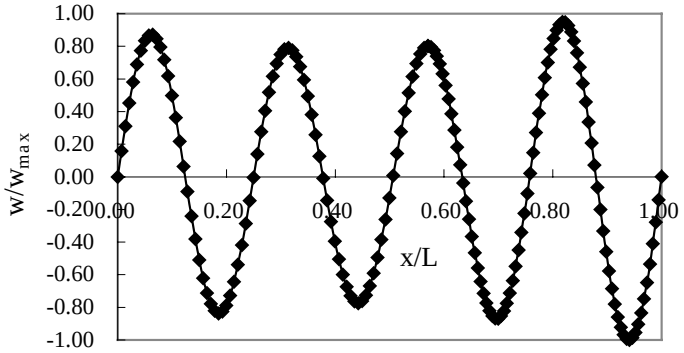

Fig. 18. The buckling mode of the specimen 1 at the instant $t = t_3$ of the second stage for the boundary condition of simple support at both ends ($\sigma_1 = 1.43\sigma_s$).

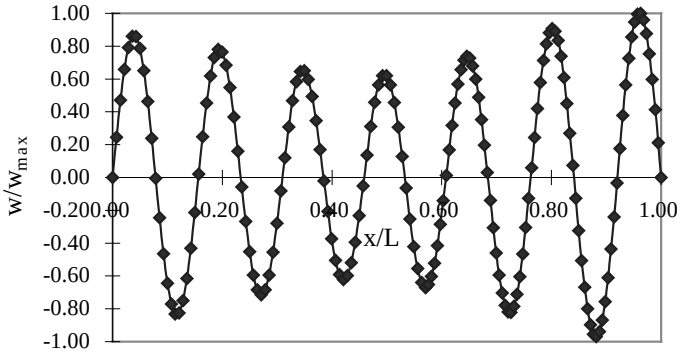

Fig. 19. The buckling mode of the specimen 17 at the instant $t = t_3$ of the second stage for the boundary condition of simple support at both ends ($\sigma_1 = 1.46\sigma_s$).

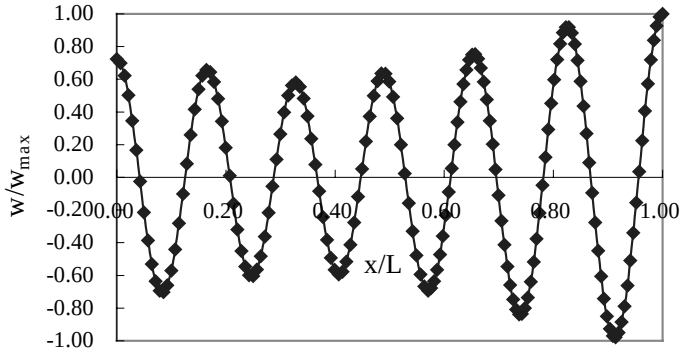

Fig. 20. The buckling mode of the specimen 17 at the instant $t = t_3$ of the second stage for the boundary condition of zero rotation and zero transverse force at both ends ($\sigma_1 = 1.36\sigma_s$).

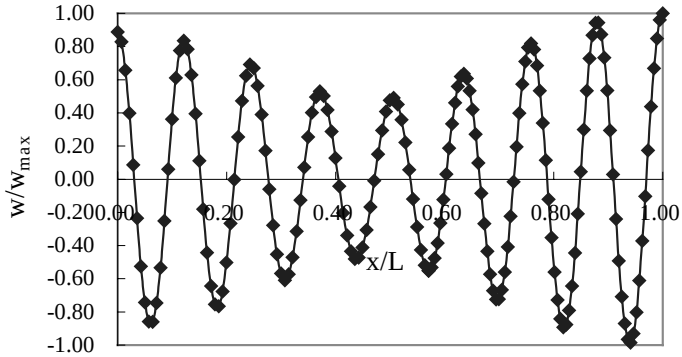

Fig. 21. The buckling mode of the specimen 23 at the instant $t = t_3$ of the second stage for the boundary condition of zero rotation and zero transverse force at both ends ($\sigma_1 = 1.33\sigma_s$).

dynamic buckling of the three specimens, which occurs at the instant $t = t_3$. The value of t_3 is given by Eq. (2.7). At the instant $t = t_3$, the reflected wave front meets with the forward plastic wave N_1, as shown in Fig. 1(d). Under the two types of restraint conditions ZRZF and SS at both ends of shells, the lowest stress ratio σ_1/σ_s that causes dynamic buckling and the corresponding deformation modes are calculated and shown in Figs. 18–21 for the three specimens. The axial half-wave numbers of the buckling modes are listed in Table 2. For the higher values of the stress ratio σ_1/σ_s, more axial half-wave numbers are obtained.

7. Conclusion

The axial critical stress and the exponential parameter of inertia terms in stability equations are treated as a couple of characteristic parameters in the present investigation on the plastic dynamic buckling of cylindrical shells under axial impact. The criterion of transformation and conservation of energy in the process of buckling initiation is used to derive the supplementary restraint equation of buckling deformation at the fronts of axial compression waves. A couple of characteristic equations for the two characteristic are derived from the conditions on which the stability equations have nontrivial solutions satisfying the boundary conditions, continuity conditions and the supplementary restraint equation. The

critical axial stress or the critical buckling time, and the exponential parameter of inertia are quantitatively calculated from the solutions of the characteristic equations.

When the axial stress resulting from impact is high, the initial buckling deformation of shells occurs in the region close to the impact end at the initial stage of compression-wave propagation. As the value of the stress ratio σ_1/σ_s increases, the critical buckling time t_{cr} decreases and the value of the characteristic parameter ω increases. When the axial stress resulting from impact is low, the initial buckling deformation of the shell may occur in the entire region of shells at the second stage of compression-wave propagation.

Acknowledgement

This work is supported by grant no. 10272114 of National Natural Science Foundation of China.

References

Brush, D.O., Almroth, B.O., 1975. Buckling of Bars, Plates and Shells. McGraw-Hill Book Company.

Budiansky, B., Hutchinson, J.W., 1964. Dynamic buckling of imperfection-sensitive structures. In: Proceedings of the 11th International Congress of Appl. Mech., Munich, West Germany.

Coppa, A.P., Nash, W.A., 1962. Dynamic buckling of shell structures subject to longitudinal impact, ASD TDR 62-744.

Fisher, C.A., Bert, C.W., 1973. Dynamic buckling of an axially compressed cylindrical shell with discrete rings and stringers. ASME Trans., J. Appl. Mech. 40, 736–740.

Florence, A.L., Goodier, J.N., 1968. Dynamic plastic buckling of cylindrical shells in sustained axial compressive flow. ASME Trans., J. Appl. Mech. 35, 80–86.

Goodier, J.N., 1967. Dynamic plastic buckling. In: Herrmann, (Ed.), Dynamic Stability of Structure, pp. 189–211.

Hutchinson, J.W., Budiansky, B., 1966. Dynamic buckling estimates. AIAA J. 4, 525–530.

Jones, N., 1989. Recent studies on the dynamic plastic behavior of structures. Appl. Mech. Rev. 42, 95–115.

Karagiozova, D., Jonse, N., 2000. Dynamic elastic–plastic buckling of circular cylindricshells under axial impact. Int. J. Solids Struct. 37, 2005–2034.

Lee, L.H.N., 1977. Quasi-bifurcation in dynamics of elastic–plastic continua. ASME Trans. J. Appl. Mech. 44, 413–418.

Lindberg, H.E., Florence, A.L., 1983. Dynamic pulse buckling-theory and experiment, Defence Nuclear Agency, Washington, Contract No. DNA 001-78-0287. Martinus Nijhoff, Norvell, MA, p. 1987.

Lindberg, H.E., Herbert, R.E., 1966. Dynamic buckling of a thin cylindrical shell under axial impact. ASME Trans., J. Appl. Mech. 33, 105–112.

Roth, R.S., Klosner, J.M., 1964. Nonlinear response of cylindrical shells with initial imperfections subjected to dynamic axial loads. AIAA paper 64-76, New York.

Simitses, G.J., 1990. Dynamic Stability of Suddenly Loaded Structures. Springer, New York.

Tamura, Y.S., Babcock, C.D., 1975. Dynamic stability of cylindrical Shells under step loading. ASME Trans., J. Appl. Mech. 42, 190–194.

Tessler, A., Tsui, T., Saether, E., 1995. A {1,2}-order theory for elasto dynamic analysis of thick orthotropic shells. Int. J. Solids Struct. 32, 3237–3260.

Lepik, Ulo, 1999. Bifurcation analysis of elastic–plastic cylindrical shells. Int. J. Non-Linear Mech. 34, 299–311.

Wang, Anwen, Tian, Wenying, 2002a. Twin-characteristic-parameter solution for dynamic buckling of columns under elastic compression wave. Int. J. Solids Struct. 39, 861–877.

Wang, Anwen, Tian, Wenying, 2002b. Characteristic-value analysis for plastic dynamic buckling of columns under elastoplastic compression waves. Int. J. Non-Linear Mech. 35, 615–628.

Wang, Lili, 1985. Foundations of Stress Waves. The Publishing House of National Defense Industry, Beijing (in Chinese).

Wang, Ren, Xiong, Zhuhua, Huang, Wenbin, 1998. Foundations of Plastic Mechanics. The Science House, Beijing (in Chinese).

Zimcik, D.G., Tennyson, R.C., 1980. Stability of circular cylindrical shells under transient axial impulsive loading. AIAA J. 18, 691–699.